Rakenteiden Mekaniikka (Journal of Structural Mechanics)
Vol. 45, No 3, 2012, pp. 133-151

Saint-Venant's torsion in intrinsic coordinates

Jukka Aalto, Juha Paavola and Eero-Matti Salonen

Abstract. Saint-Venant's torsion is considered in the so-called intrinsic coordinates. Warping function formulation is applied. Certain relations are derived for a rather general geometry. In connection with thin-walled open cross-sections an inconsistency is discussed. A weak form suitable for solution by the finite element method is presented. Numerical examples using linear triangular finite elements are finally worked out to demonstrate the efficiency of the new formulation.

Key words: Saint-Venant torsion, intrinsic coordinates, thin-walled open section, weak form

Introduction

Figure 1(a) shows the η,ζ-coordinate system employed in this article. Quantity ζ is the directed arc length along a fixed line (we call it here as the spine) in a plane. Quantity η is the directed perpendicular distance (defined here positive when it is obtained by rotation in the clockwise direction from the positive direction of ζ) from the spine to a generic point Q in the plane. The corresponding unit base vectors are $\mathbf{e}_\eta$ and $\mathbf{e}_\zeta$ The curvature $1/R$ of the spine is defined here as positive if the center of curvature K is on the negative η-axis side. The coordinate system is orthogonal and curvilinear (if the spine is curved). Figure 1(b) shows a typical application of the system in structural mechanics. Here the figure could present a curved plane beam with the spine as the beam axis. Alternatively, the figure could describe a cross-section of a thin-walled rod the spine following some middle line of the section. This is one interpretation used in the present article. In fluid mechanics the η,ζ-coordinate system is employed in the study of boundary layer flow in the vicinity of a solid surface. The spine is then attached to the body surface and the coordinate η is directed into the fluid. In [1] the name body intrinsic coordinates is used in this connection. Although the η,ζ-coordinate system is employed quite frequently in structural mechanics, rather surprisingly, no standard name seems to be in use for it. We will call the system simply as the intrinsic coordinate system (in Finnish rankakoordinaatisto). In basic engineering mathematics courses some orthogonal curvilinear coordinate systems such as the polar or spherical system are usually dealt with. However, the intrinsic system is not normally included. A rather systematic way to deal with orthogonal curvilinear coordinates in general is described in the articles [2], [3] and [4] including also the intrinsic system as a special case.

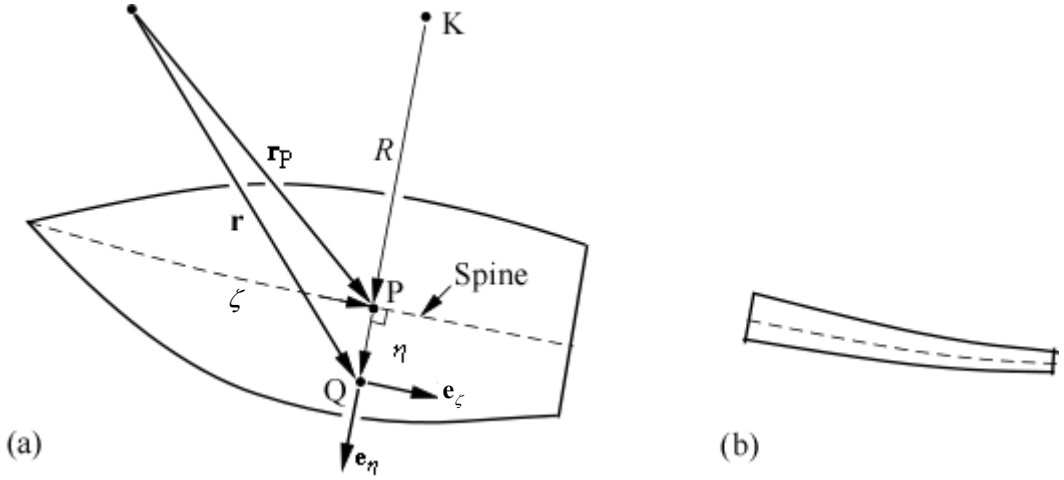

Figure 1 (a) Intrinsic coordinates and the corresponding unit base vectors. (b) A thin geometry.

It is obvious that the intrinsic system puts some constraints on the geometry that can be dealt with it. First, the domain considered must not exceed the perpendicular lines to the end-points of the spine. Second, the centres of curvature for the spine must be outside the domain. Thus, the intrinsic coordinate system is clearly suitable for more or less weakly distorted rectangular domains. However, with them it is the most preferable system.

The position vector of a generic point Q is (Figure 1(a))

$$\mathbf{r}(\eta,\zeta)=\mathbf{r}_P(\zeta)+\eta\mathbf{e}_\eta(\zeta), \tag{1}$$

where P is a corresponding generic point on the spine. From curve theory,

$$\frac{\mathrm{d}\mathbf{r}_P}{\mathrm{d}\zeta}=\mathbf{e}_\zeta \tag{2}$$

and the well-known Frenet formulae give

$$\frac{\mathrm{d}\mathbf{e}_\eta}{\mathrm{d}\zeta}=\frac{1}{R}\mathbf{e}_\zeta, \quad \frac{\mathrm{d}\mathbf{e}_\zeta}{\mathrm{d}\zeta}=-\frac{1}{R}\mathbf{e}_\eta. \tag{3}$$

Differentiation of (1) gives

$$\begin{aligned}\frac{\partial\mathbf{r}}{\partial\eta}&=\mathbf{e}_\eta,\\ \frac{\partial\mathbf{r}}{\partial\zeta}&=\frac{\mathrm{d}\mathbf{r}_P}{\mathrm{d}\zeta}+\eta\frac{\mathrm{d}\mathbf{e}_\eta}{\mathrm{d}\zeta}=\mathbf{e}_\zeta+\eta\frac{\mathbf{e}_\zeta}{R}=\left(1+\frac{\eta}{R}\right)\mathbf{e}_\zeta.\end{aligned} \tag{4}$$

From these formulas follow the so-called scale factors

$$h_\eta=1, \quad h_\zeta=1+\frac{\eta}{R}. \tag{5}$$

Displacements and strains

Figure 2 shows some details of a rod cross-section with the rod axis parallel to the x-axis. The rod is assumed to be under Saint-Venant's torsion [5]. It is convenient to employ here vector notations. The displacement of point Q is represented by

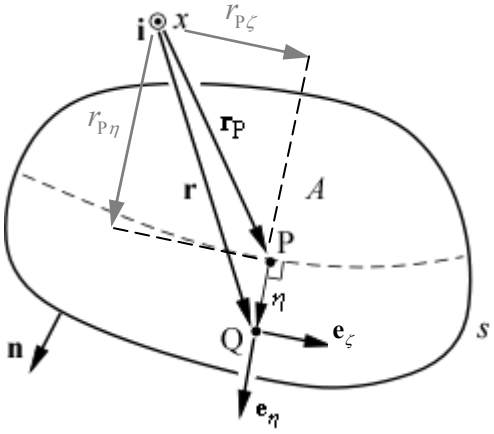

Figure 2. Cross-section of a rod and some notations.

$$\mathbf{u} = u_x\mathbf{i} + u_\eta\mathbf{e}_\eta + u_\zeta\mathbf{e}_\zeta . \tag{6}$$

The axial displacement component is given by the warping function $\psi = \psi(\eta,\zeta)$ as

$$u_x = \theta\psi , \tag{7}$$

where θ is the rate of twist. The displacement in the cross-sectional plane due to the (small) rotation $\theta x\mathbf{i}$ of the cross-section is obtained by the vector cross product (The rotation center is assumed to be at the origin of the position vector and it has been assumed that the rotation is zero at $x = 0$)

$$\theta x\mathbf{i}\times\mathbf{r} . \tag{8}$$

Thus, the corresponding displacement components are

$$u_\eta = \theta x\left(\mathbf{i}\times\mathbf{r}\right)\bullet\mathbf{e}_\eta , \tag{9}$$

$$u_\zeta = \theta x\left(\mathbf{i}\times\mathbf{r}\right)\bullet\mathbf{e}_\zeta . \tag{10}$$

Using expression (1) and taking into account the rules of the scalar triple product and the cross product gives

$$u_\eta = \theta x\left(\mathbf{e}_\eta\times\mathbf{i}\right)\bullet\left(\mathbf{r}_P + \eta\mathbf{e}_\eta\right) = \theta x\left(-\mathbf{e}_\zeta\right)\bullet\left(\mathbf{r}_P + \eta\mathbf{e}_\eta\right) = -\theta x r_{P\zeta} , \tag{11}$$

$$u_\zeta = \theta x\left(\mathbf{e}_\zeta\times\mathbf{i}\right)\bullet\left(\mathbf{r}_P + \eta\mathbf{e}_\eta\right) = \theta x\left(\mathbf{e}_\eta\right)\bullet\left(\mathbf{r}_P + \eta\mathbf{e}_\eta\right) = \theta x\left(r_{P\eta} + \eta\right), \tag{12}$$

where

$$r_{P\eta} = \mathbf{e}_\eta\bullet\mathbf{r}_P , \qquad r_{P\zeta} = \mathbf{e}_\zeta\bullet\mathbf{r}_P . \tag{13}$$

Here $r_{\mathrm{P}\eta}$ and $r_{\mathrm{P}\zeta}$ are the components of position vector $\mathbf{r}_{\mathrm{P}}$ in $\eta-$ and $\zeta-$directions in the physical plane (see Figure 2).

The only non-zero strains are shearing strain components $\gamma_{x\eta}$ and $\gamma_{x\zeta}$ with formulas (can be derived e.g. by the method described in [3])

$$\gamma_{x\eta} = \frac{\partial u_x}{\partial \eta} + \frac{\partial u_\eta}{\partial x}, \tag{14}$$

$$\gamma_{x\zeta} = \frac{1}{1+\eta/R}\frac{\partial u_x}{\partial \zeta} + \frac{\partial u_\zeta}{\partial x}. \tag{15}$$

Substituting expressions (7), (11) and (12) gives

$$\gamma_{x\eta} = \theta\left(\frac{\partial \psi}{\partial \eta} - r_{\mathrm{P}\zeta}\right), \tag{16}$$

$$\gamma_{x\zeta} = \theta\left(\frac{1}{1+\eta/R}\frac{\partial \psi}{\partial \zeta} + r_{\mathrm{P}\eta} + \eta\right). \tag{17}$$

Equilibrium

Assuming homogeneous linear elastic material with shearing modulus G, the only non-zero stresses are the shearing stress components

$$\tau_{x\eta} = G\gamma_{x\eta} = G\theta\left(\frac{\partial \psi}{\partial \eta} - r_{\mathrm{P}\zeta}\right), \tag{18}$$

$$\tau_{x\zeta} = G\gamma_{x\zeta} = G\theta\left(\frac{1}{1+\eta/R}\frac{\partial \psi}{\partial \zeta} + r_{\mathrm{P}\eta} + \eta\right). \tag{19}$$

The stress equilibrium equation is found to become (can be derived e.g. by the method described in [3])

$$\frac{\partial}{\partial \eta}\left[\left(1+\frac{\eta}{R}\right)\tau_{x\eta}\right] + \frac{\partial \tau_{x\zeta}}{\partial \zeta} = 0 \quad \text{in } A. \tag{20}$$

The traction boundary condition is

$$n_\eta \tau_{x\eta} + n_\zeta \tau_{x\zeta} = 0 \quad \text{on } s. \tag{21}$$

where n_η and n_ζ are the components of the unit outward normal vector $\mathbf{n} = n_\eta \mathbf{e}_\eta + n_\zeta \mathbf{e}_\zeta$.

Using (18) and (19) in (20) and (21), there is obtained the differential equation

$$\frac{\partial}{\partial \eta}\left[\left(1+\frac{\eta}{R}\right)\left(\frac{\partial \psi}{\partial \eta} - r_{\mathrm{P}\zeta}\right)\right] + \frac{\partial}{\partial \zeta}\left(\frac{1}{1+\eta/R}\frac{\partial \psi}{\partial \zeta} + r_{\mathrm{P}\eta} + \eta\right) = 0 \quad \text{in } A \tag{22}$$

and the corresponding boundary condition

$$n_\eta\left(\frac{\partial\psi}{\partial\eta}-r_{\mathrm{P}\zeta}\right)+n_\zeta\left(\frac{1}{1+\eta/R}\frac{\partial\psi}{\partial\zeta}+r_{\mathrm{P}\eta}+\eta\right)=0\quad\text{on } s\,. \tag{23}$$

Differentiation of (13a) gives

$$\frac{\partial r_{\mathrm{P}\eta}}{\partial\zeta}=\frac{\partial\mathbf{e}_\eta}{\partial\zeta}\bullet\mathbf{r}_\mathrm{P}+\mathbf{e}_\eta\bullet\frac{\partial\mathbf{r}_\mathrm{P}}{\partial\zeta}=\frac{1}{R}\mathbf{e}_\zeta\bullet\mathbf{r}_\mathrm{P}+\mathbf{e}_\eta\bullet\mathbf{e}_\zeta=\frac{r_{\mathrm{P}\zeta}}{R}\,. \tag{24}$$

After some manipulation and using the result (24), equations (22) and (23) reduce to

$$\frac{\partial}{\partial\eta}\left[\left(1+\frac{\eta}{R}\right)\frac{\partial\psi}{\partial\eta}\right]+\frac{\partial}{\partial\zeta}\left(\frac{1}{1+\eta/R}\frac{\partial\psi}{\partial\zeta}\right)=0\quad\text{in } A \tag{25}$$

and

$$n_\eta\frac{\partial\psi}{\partial\eta}+n_\zeta\frac{1}{1+\eta/R}\frac{\partial\psi}{\partial\zeta}=n_\eta r_{\mathrm{P}\zeta}-n_\zeta\left(r_{\mathrm{P}\eta}+\eta\right)\quad\text{on } s\,. \tag{26}$$

Equations (25) and (26) form the boundary value problem for the warping function ψ in its simplest form. Equations (22) and (22) are, however, used as starting point for the corresponding weak form in the following.

Twisting moment

The moment vector with respect to origin of the position vector is (Figure 2)

$$\mathbf{M}=\int_A\mathbf{r}\times\left(\tau_{x\eta}\mathbf{e}_\eta+\tau_{x\zeta}\mathbf{e}_\zeta\right)\mathrm{d}A\,. \tag{27}$$

Integrating this over the corresponding domain in the ξ,η-plane produces the form

$$\mathbf{M}=\int_{\eta,\zeta}\mathbf{r}\times\left(\tau_{x\eta}\mathbf{e}_\eta+\tau_{x\zeta}\mathbf{e}_\zeta\right)\left(1+\frac{\eta}{R}\right)\mathrm{d}\eta\mathrm{d}\zeta\,. \tag{28}$$

The term $1+\eta/R$ comes from the relation $\mathrm{d}A=h_\eta h_\zeta\mathrm{d}\eta\mathrm{d}\zeta=(1+\eta/R)\mathrm{d}\eta\mathrm{d}\zeta$. The corresponding scalar twisting moment is

$$T=\mathbf{M}\bullet\mathbf{i}=\int_{\eta,\zeta}\mathbf{r}\times\left(\tau_{x\eta}\mathbf{e}_\eta+\tau_{x\zeta}\mathbf{e}_\zeta\right)\bullet\mathbf{i}\left(1+\frac{\eta}{R}\right)\mathrm{d}\eta\mathrm{d}\zeta\,. \tag{29}$$

Applying again the rules of scalar triple product and some further manipulation gives next

$$\begin{aligned}T&=\int_{\eta,\zeta}\mathbf{r}\bullet\left[\left(\tau_{x\eta}\mathbf{e}_\eta+\tau_{x\zeta}\mathbf{e}_\zeta\right)\times\mathbf{i}\right]\left(1+\frac{\eta}{R}\right)\mathrm{d}\eta\mathrm{d}\zeta\\&=\int_{\eta,\zeta}\mathbf{r}\bullet\left(\tau_{x\zeta}\mathbf{e}_\eta-\tau_{x\eta}\mathbf{e}_\zeta\right)\left(1+\frac{\eta}{R}\right)\mathrm{d}\eta\mathrm{d}\zeta\,.\end{aligned} \tag{30}$$

When formula (1) is used this becomes

$$T = \int_{\eta,\zeta} \left[\left(r_{\mathrm{P}\eta} + \eta \right) \tau_{x\zeta} - r_{\mathrm{P}\zeta} \tau_{x\eta} \right] \left(1 + \frac{\eta}{R} \right) \mathrm{d}\eta \mathrm{d}\zeta \,. \tag{31}$$

Now the value of the twisting moment should not depend on $\mathbf{r}_{\mathrm{P}}$. This is difficult to see directly from (31). Further, vector $\mathbf{r}_{\mathrm{P}}$ appears in the boundary condition (23) and the solution for ψ obviously changes if the origin of $\mathbf{r}_{\mathrm{P}}$ is changed; that is, $\mathbf{r}_{\mathrm{P}}$ changes. This is in principle correct as it is known from the theory that ψ can be altered by a rigid body motion without changing the deformations and the stresses.

We will demonstrate here that (31) is invariant with respect to the selection of the origin of $\mathbf{r}_{\mathrm{P}}$. Instead of studying directly expression (31) we will show that the resultant of the stresses on the cross-section

$$\mathbf{Q} = \int_{\eta,\zeta} \left(\tau_{x\zeta} \mathbf{e}_\zeta + \tau_{x\eta} \mathbf{e}_\eta \right) \left(1 + \frac{\eta}{R} \right) \mathrm{d}\eta \mathrm{d}\zeta \tag{32}$$

vanishes, which shows that the twisting moment cannot depend on the selection of origin of the radius vector.

For the proof we will need the integration by parts formulas in intrinsic coordinates. These will be useful also later in this article. For two functions $f(\eta,\xi)$ and $g(\eta,\zeta)$ the formulas read in intrinsic coordinates, e.g. [2],

$$\int_{\eta,\zeta} f \frac{\partial g}{\partial \eta} \mathrm{d}\eta \mathrm{d}\zeta = -\int_{\eta,\zeta} \frac{\partial f}{\partial \eta} g \, \mathrm{d}\eta \mathrm{d}\zeta + \int_s \frac{n_\eta}{1 + \eta / R} f g \mathrm{d}s \,, \tag{33}$$

$$\int_{\eta,\zeta} f \frac{\partial g}{\partial \zeta} \mathrm{d}\eta \mathrm{d}\zeta = -\int_{\eta,\zeta} \frac{\partial f}{\partial \zeta} g \, \mathrm{d}\eta \mathrm{d}\zeta + \int_s n_\zeta f g \mathrm{d}s \,. \tag{34}$$

It should be noticed that the area integrals are over the transformed domain in the η,ζ-plane but the boundary integrals are over the boundary in the original geometry.

Some manipulations on equilibrium equation (20) follow. Both sides of it are multiplied by $\mathbf{r}$ and both sides of the resulting equation are integrated directly over the corresponding domain the ξ,η-plane:

$$\int_{\eta,\zeta} \left\{ \frac{\partial}{\partial \eta} \left[\left(1 + \frac{\eta}{R} \right) \tau_{x\eta} \right] \mathbf{r} + \frac{\partial \tau_{x\zeta}}{\partial \zeta} \mathbf{r} \right\} \mathrm{d}\eta \, \mathrm{d}\zeta = \mathbf{0} \,. \tag{35}$$

Integrating by parts gives first

$$-\int_{\eta,\zeta} \left\{ \left[\left(1 + \frac{\eta}{R} \right) \tau_{x\eta} \right] \frac{\partial \mathbf{r}}{\partial \eta} + \tau_{x\zeta} \frac{\partial \mathbf{r}}{\partial \zeta} \right\} \mathrm{d}\eta \mathrm{d}\zeta$$
$$+\int_s \left(n_\eta \tau_{x\eta} \mathbf{r} + n_\zeta \tau_{x\zeta} \mathbf{r} \right) \mathrm{d}s = \mathbf{0} \,. \tag{36}$$

Taking into account formulas (4) and after some arrangement:

$$-\int_{\eta,\zeta} \left\{ \left(1 + \frac{\eta}{R} \right) \tau_{x\eta} \mathbf{e}_\eta + \tau_{x\zeta} \left(1 + \frac{\eta}{R} \right) \mathbf{e}_\zeta \right\} \mathrm{d}\eta \, \mathrm{d}\zeta$$
$$+\int_s \left(n_\eta \tau_{x\eta} + n_\zeta \tau_{x\zeta} \right) \mathbf{r} \, \mathrm{d}s = \mathbf{0} \,. \tag{37}$$

The line integral disappears by the traction boundary condition (21) and expression (32) is thus seen to vanish.

An important property of a twisted cross-section is the torsional constant J, which is defined by the equation

$$T = GJ\theta\,. \tag{38}$$

In order to determine it, the warping function $\psi(\eta,\zeta)$ as a solution of the boundary value problem of equations (22) and (23) is needed. Substituting the shearing stresses (18) and (19) into (31) and comparing the result with(38) results to

$$J = \int_{\eta,\zeta}\left[\left(r_{\mathrm{P}\eta}+\eta\right)\left(\frac{1}{1+\eta/R}\frac{\partial\psi}{\partial\zeta}+r_{\mathrm{P}\eta}+\eta\right)-r_{\mathrm{P}\zeta}\left(\frac{\partial\psi}{\partial\eta}-r_{\mathrm{P}\zeta}\right)\right]\left(1+\frac{\eta}{R}\right)\mathrm{d}\eta\mathrm{d}\zeta \tag{39}$$

for the torsional constant. This can be applied for determining the torsional constant after a finite element solution for the warping function has been found.

Typical problem in practice is to determine the distribution of the shearing stresses $\tau_{x\eta}(\eta,\zeta)$ and $\tau_{x\zeta}(\eta,\zeta)$ corresponding to a given value of the twisting moment T. Simple formulas for doing this are obtained using (18), (19) and (38):

$$\tau_{x\eta} = \frac{T}{J}\left(\frac{\partial\psi}{\partial\eta}-r_{\mathrm{P}\zeta}\right), \tag{40}$$

$$\tau_{x\zeta} = \frac{T}{J}\left(\frac{1}{1+\eta/R}\frac{\partial\psi}{\partial\zeta}+r_{\mathrm{P}\eta}+\eta\right). \tag{41}$$

An alternative formula for the twisting moment

We will derive an alternative formula for the twisting moment using the notations of Figure 3. For this geometry the integration over the cross-section can be performed conveniently by double integrations.

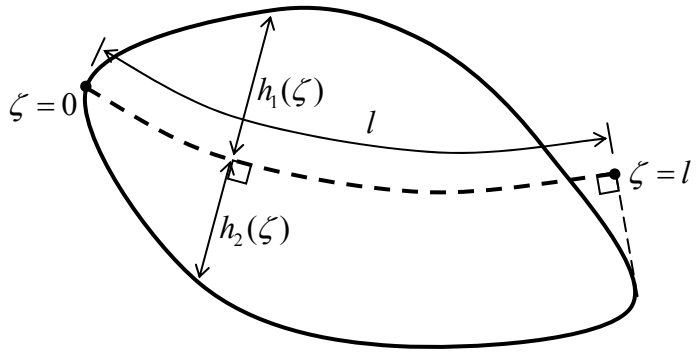

Figure 3. Some notations.

The twisting moment (31) is written first as

$$T = \int_{\eta,\zeta} \left[\eta + r_{\mathrm{P}\eta} \left(1 + \frac{\eta}{R} \right) + \frac{\eta^2}{R} \right] \tau_{x\zeta} \, \mathrm{d}\eta \mathrm{d}\zeta - \int_{\eta,\zeta} r_{\mathrm{P}\zeta} \tau_{x\eta} \left(1 + \frac{\eta}{R} \right) \mathrm{d}\eta \mathrm{d}\zeta \, . \qquad (42)$$

In thin geometries non-zero stresses $\tau_{x\eta}$ appear mainly near the cross-section ends and are difficult to approximate. We therefore now try to get rid of the last integral in (42).

We multiply both sides of equation (20) by the term $r_{\mathrm{P}\zeta} R$ and integrate over A and transform over the domain in the ξ, η -plane:

$$\int_{\eta,\zeta} \frac{\partial \tau_{x\zeta}}{\partial \zeta} r_{\mathrm{P}\zeta} R \left(1 + \frac{\eta}{R} \right) \mathrm{d}\eta \mathrm{d}\zeta + \int_{\eta,\zeta} \frac{\partial}{\partial \eta} \left[\left(1 + \frac{\eta}{R} \right) \tau_{x\eta} \right] r_{\mathrm{P}\zeta} R \left(1 + \frac{\eta}{R} \right) \mathrm{d}\eta \mathrm{d}\zeta = 0 \, . \qquad (43)$$

Application of integration by parts formulas (33) and (34) gives

$$\begin{aligned} &- \int_{\eta,\zeta} \tau_{x\zeta} \frac{\partial}{\partial \xi} \left[r_{\mathrm{P}\zeta} R \left(1 + \frac{\eta}{R} \right) \right] \mathrm{d}\eta \mathrm{d}\zeta + \int_s n_\zeta \tau_{x\zeta} r_{\mathrm{P}\zeta} R \left(1 + \frac{\eta}{R} \right) \mathrm{d}s \\ &- \int_{\eta,\zeta} \tau_{x\eta} \left(1 + \frac{\eta}{R} \right) \frac{\partial}{\partial \eta} \left[r_{\mathrm{P}\zeta} R \left(1 + \frac{\eta}{R} \right) \right] \mathrm{d}\eta \mathrm{d}\zeta + \int_s n_\eta \tau_{x\eta} r_{\mathrm{P}\zeta} R \left(1 + \frac{\eta}{R} \right) \mathrm{d}s = 0 \, . \end{aligned} \qquad (44)$$

Next we have

$$\begin{aligned} &- \int_{\eta,\zeta} \tau_{x\zeta} \left[\frac{\mathrm{d}r_{\mathrm{P}\zeta}}{\mathrm{d}\zeta} (R + \eta) + r_{\mathrm{P}\zeta} \frac{\mathrm{d}R}{\mathrm{d}\zeta} \right] \mathrm{d}\eta \mathrm{d}\zeta - \int_{\eta,\zeta} \tau_{x\eta} \left(1 + \frac{\eta}{R} \right) \left[r_{\mathrm{P}\zeta} R \frac{1}{R} \right] \mathrm{d}\eta \mathrm{d}\zeta \\ &\qquad + \int_s \left(n_\eta \tau_{x\eta} + n_\zeta \tau_{x\zeta} \right) r_{\mathrm{P}\zeta} R \left(1 + \frac{\eta}{R} \right) \mathrm{d}s = 0 \, . \end{aligned} \qquad (45)$$

The line integral disappears by the traction boundary condition. Further,

$$\frac{\mathrm{d}r_{\mathrm{P}\zeta}}{\mathrm{d}\zeta} = \frac{\mathrm{d}}{\mathrm{d}\zeta} \left(\mathbf{r}_\mathrm{P} \bullet \mathbf{e}_\zeta \right) = \frac{\mathrm{d}\mathbf{r}_\mathrm{P}}{\mathrm{d}\zeta} \bullet \mathbf{e}_\zeta + \mathbf{r}_\mathrm{P} \bullet \frac{\mathrm{d}\mathbf{e}_\zeta}{\mathrm{d}\zeta} = \mathbf{e}_\zeta \bullet \mathbf{e}_\zeta + \mathbf{r}_\mathrm{P} \bullet \left(-\frac{1}{R} \mathbf{e}_\eta \right) = 1 - \frac{r_{\mathrm{P}\eta}}{R} \, . \qquad (46)$$

Thus, (45) becomes

$$- \int_{\eta,\zeta} \tau_{x\zeta} \left[\left(1 - \frac{r_{\mathrm{P}\eta}}{R} \right) (R + \eta) + r_{\mathrm{P}\zeta} \frac{\mathrm{d}R}{\mathrm{d}\zeta} \right] \mathrm{d}\eta \mathrm{d}\zeta - \int_{\eta,\zeta} \tau_{x\eta} \left(1 + \frac{\eta}{R} \right) r_{\mathrm{P}\zeta} \, \mathrm{d}\eta \mathrm{d}\zeta = 0 \, . \qquad (47)$$

From this, the needed term is

$$- \int_{\eta,\zeta} r_{\mathrm{P}\zeta} \tau_{x\eta} \left(1 + \frac{\eta}{R} \right) \mathrm{d}\eta \mathrm{d}\zeta = \int_{\eta,\zeta} \left[r_{\mathrm{P}\zeta} \frac{\mathrm{d}R}{\mathrm{d}\zeta} + R + \eta - r_{\mathrm{P}\eta} \left(1 + \frac{\eta}{R} \right) \right] \tau_{x\zeta} \, \mathrm{d}\eta \mathrm{d}\zeta \, . \qquad (48)$$

The twisting moment (42) obtains the form

$$T = \int_{\eta,\zeta} \left(r_{\mathrm{P}\zeta} \frac{\mathrm{d}R}{\mathrm{d}\zeta} + R \right) \tau_{x\zeta} \, \mathrm{d}\eta \mathrm{d}\zeta + \int_{\eta,\zeta} \left(2\eta + \frac{\eta^2}{R} \right) \tau_{x\zeta} \, \mathrm{d}\eta \mathrm{d}\zeta \, . \qquad (49)$$

Expressing the first integral term using a double integral we get

$$T=\int_0^l\left[\left(r_{\mathrm{P}\zeta}\frac{\mathrm{d}R}{\mathrm{d}\zeta}+R\right)\int_{-h_1}^{h_2}\tau_{x\zeta}\mathrm{d}\eta\right]\mathrm{d}\zeta+\int_{\eta,\zeta}\left(2\eta+\frac{\eta^2}{R}\right)\tau_{x\zeta}\,\mathrm{d}\eta\mathrm{d}\zeta\,. \tag{50}$$

From Appendix A it follows that here

$$\int_{-h_1}^{h_2}\tau_{x\zeta}\mathrm{d}\eta=0\,. \tag{51}$$

Using this result, (50) simplifies to

$$T=\int_{\eta,\zeta}\left(2\eta+\frac{\eta^2}{R}\right)\tau_{x\zeta}\mathrm{d}\eta\mathrm{d}\zeta\,. \tag{52}$$

Based on equation (52) of the twisting moment, an alternative formula for the torsional constant, which can be used in connection with the specific geometry of Figure 3, can be obtained. Substituting the shearing stress (19) into (52) and comparing the result with (38) gives

$$J=\int_{\eta,\zeta}\left(2\eta+\frac{\eta^2}{R}\right)\left(\frac{1}{1+\eta/R}\frac{\partial\psi}{\partial\zeta}+r_{\mathrm{P}\eta}+\eta\right)\mathrm{d}\eta\mathrm{d}\zeta\,. \tag{53}$$

This can be used as an alternative formula for determining the torsional constant J after the warping function has been determined.

Formula (52) is interesting when applied to thin-walled sections. Making the standard approximation $\tau_{x\zeta}=2G\theta\eta$, ($\tau_{x\eta}=0$) and noting that $h_1=h_2=t/2$, gives the correct twisting moment

$$T=\frac{1}{3}G\theta\int_0^l t^3\mathrm{d}\zeta\,. \tag{54}$$

If, however, formula (31) is used as a starting point, an erroneous expression

$$T=\frac{1}{6}G\theta\int_0^l(1+\frac{r_{\mathrm{P}\eta}}{R})t^3\mathrm{d}\zeta \tag{55}$$

emerges. This can be compared to the results obtained in [5] on page 274 for a narrow rectangular section and the associated explanation.

We note finally that equation (51) is valid even if the cross-section has, say holes, and we still can arrive at (52) and (53).

Weak form

For applications of the finite element method we will derive an appropriate weak form. Multiplying both sides of (22) by a weighting function $\delta\psi=w$ and integrating over the domain in the η,ζ- plane gives an initial weak form

$$\int_{\eta,\zeta}w\left\{\frac{\partial}{\partial\eta}\left[\left(1+\frac{\eta}{R}\right)\left(\frac{\partial\psi}{\partial\eta}-r_{\mathrm{P}\xi}\right)\right]+\frac{\partial}{\partial\zeta}\left(\frac{1}{1+\eta/R}\frac{\partial\psi}{\partial\zeta}+r_{\mathrm{P}\eta}+\eta\right)\right\}\mathrm{d}\eta\mathrm{d}\zeta=0\,. \tag{56}$$

Integration by parts formulas (33) and (34) are applied. The result is first

$$\begin{aligned}&\int_s w\left\{n_\eta\left(\frac{\partial\psi}{\partial\eta}-r_{\mathrm{P}\zeta}\right)+n_\zeta\left(\frac{1}{1+\eta/R}\frac{\partial\psi}{\partial\zeta}+r_{\mathrm{P}\eta}+\eta\right)\right\}\mathrm{d}s\\&-\int_{\eta,\zeta}\left\{\frac{\partial w}{\partial\eta}\left[\left(1+\frac{\eta}{R}\right)\left(\frac{\partial\psi}{\partial\eta}-r_{\mathrm{P}\zeta}\right)+\frac{\partial w}{\partial\zeta}\left(\frac{1}{1+\eta/R}\frac{\partial\psi}{\partial\zeta}+r_{\mathrm{P}\eta}+\eta\right)\right]\right\}\mathrm{d}\eta\mathrm{d}\zeta=0.\end{aligned}\tag{57}$$

The line integral term disappears by the boundary condition (23) and the final weak form is

$$\begin{aligned}&\int_{\eta,\zeta}\left[\left(1+\frac{\eta}{R}\right)\frac{\partial w}{\partial\eta}\frac{\partial\psi}{\partial\eta}+\frac{1}{1+\eta/R}\frac{\partial w}{\partial\zeta}\frac{\partial\psi}{\partial\zeta}\right]\mathrm{d}\eta\mathrm{d}\zeta\\&=\int_{\eta,\zeta}\left[\frac{\partial w}{\partial\eta}\left(1+\frac{\eta}{R}\right)r_{\mathrm{P}\zeta}-\frac{\partial w}{\partial\zeta}\left(r_{\mathrm{P}\eta}+\eta\right)\right]\mathrm{d}\eta\mathrm{d}\zeta=0.\end{aligned}\tag{58}$$

As only derivatives of ψ appear, the level of ψ must be fixed for instance by giving the value of ψ at one nodal point.

Example cases

A finite element program based on the weak form (58) was developed in this work in MATLAB environment by the first writer. The program uses linear triangles and integrations over the elements are performed numerically. In order to get smooth shearing stresses for visualization, single valued nodal values are obtained by averaging the consistent shearing stresses of the corresponding element nodes. A comparison of the results of the present formulation and of the standard finite element formulation is done in the examples to follow. Therefore a corresponding finite element program using linear triangles was also developed.

Annular cross-section with a sectorial cut (Figure 4) was studied as a first example. The spine of the intrinsic coordinate system follows the circular center line of the cross section. Figures 5 and 6 show typical grids of linear triangular elements of the intrinsic coordinate finite element formulation (intrinsic formulation) and the standard finite element formulation (standard formulation), respectively. Figures 7 and 8 show distribution of the resultant shearing stress τ obtained with the intrinsic and standard formulations, respectively. Table 1 shows comparison the maximum shearing stress $\tau_{\max}$ obtained with the two formulations using different mesh densities. Table 2 shows similar comparison of the torsional constant J. Practically exact results shown in Tables 1 and 2 were obtained with the standard formulation using a very dense mesh (32×160) of biquadratic iso-parametric quadrilateral elements.

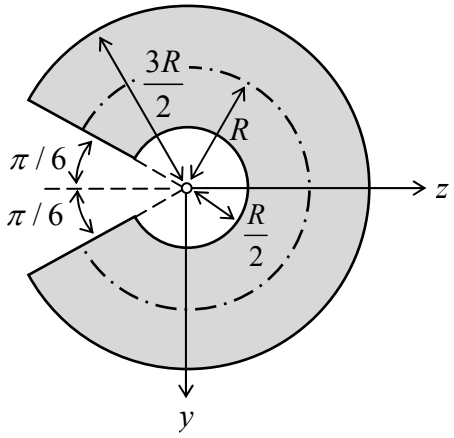

Figure 4. Annular cross-section with a sectorial cut.

Table 1. Comparison of the values of dimensionless maximum shearing stress $\tau_{\max} / TR^3$, annular cross-section with a cut.

Element division	Intrinsic formulation	Standard formulation
1×5	0,814	0,619
2×10	0,789	0,507
4×20	0,814	0,664
8×40	0,833	0,754
16×80	0,842	0,801
32×160	0,845	0,824
Practically exact result 0,848		

Table 2. Comparison of the values of dimensionless torsional constant J / R^4, annular cross-section with a cut.

Element division	Intrinsic formulation	Standard formulation
1×5	1,76	1,90
2×10	1,67	1,77
4×20	1,59	1,63
8×40	1,56	1,57
16×80	1,56	1,56
32×160	1,56	1,56
Practically exact result 1,55		

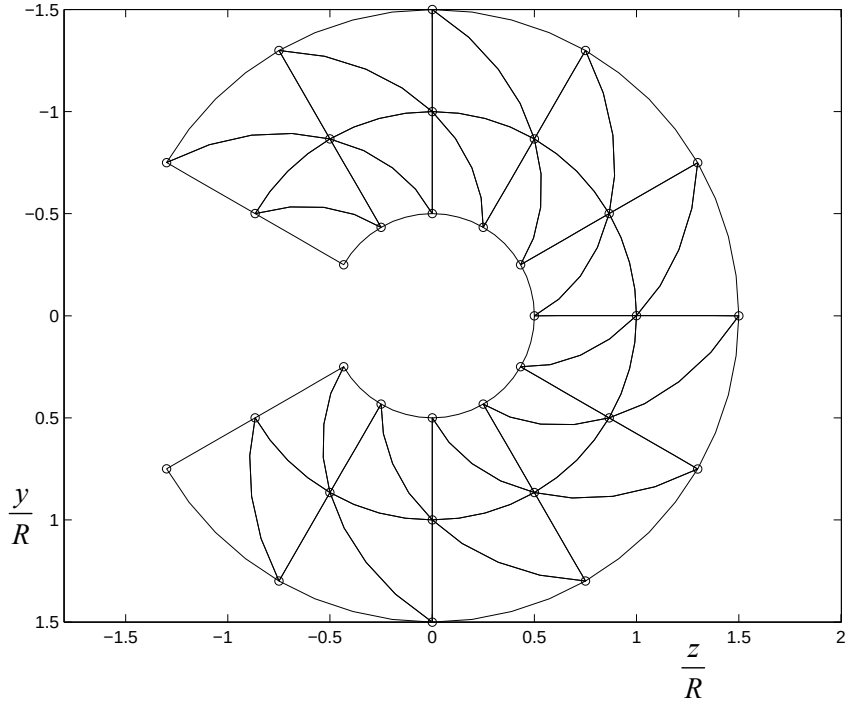

Figure 5. Typical mesh of linear triangles of the intrinsic formulation.

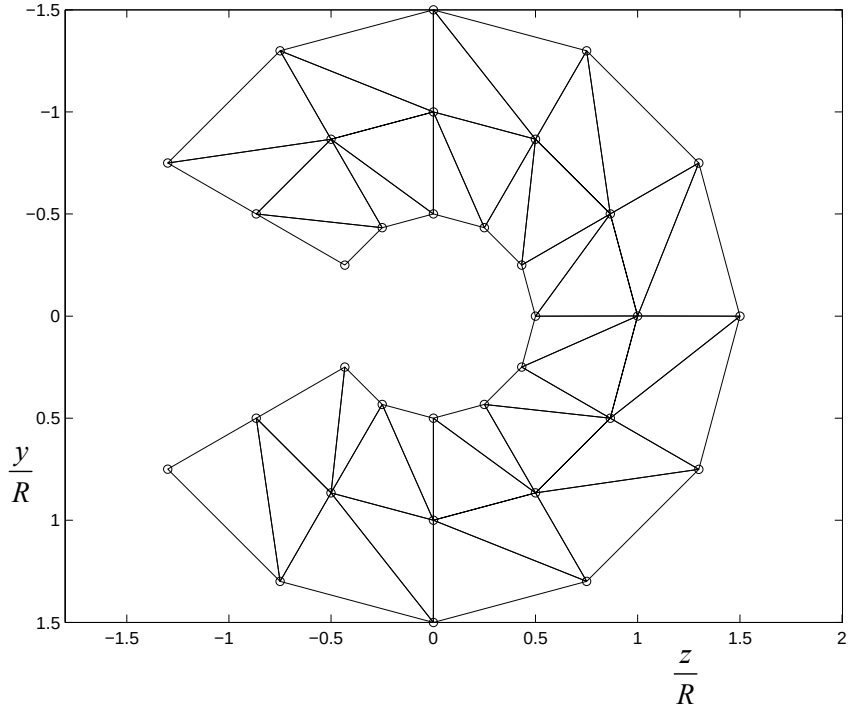

Figure 6. Typical mesh of linear triangles of the standard formulation.

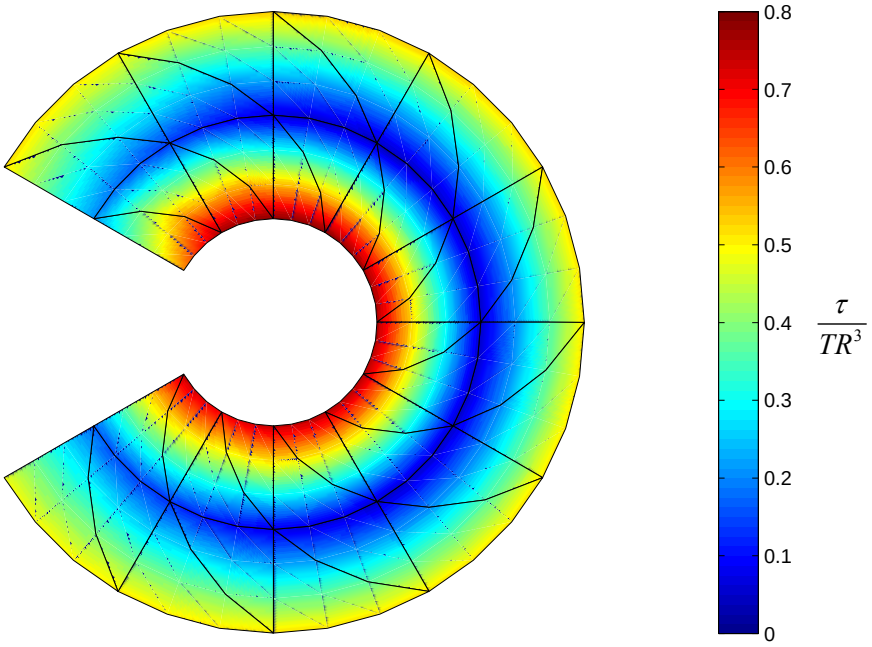

Figure 7. Distribution of the resultant shearing stress $\tau = \sqrt{\tau_{x\xi}^2 + \tau_{x\eta}^2}$, intrinsic formulation.

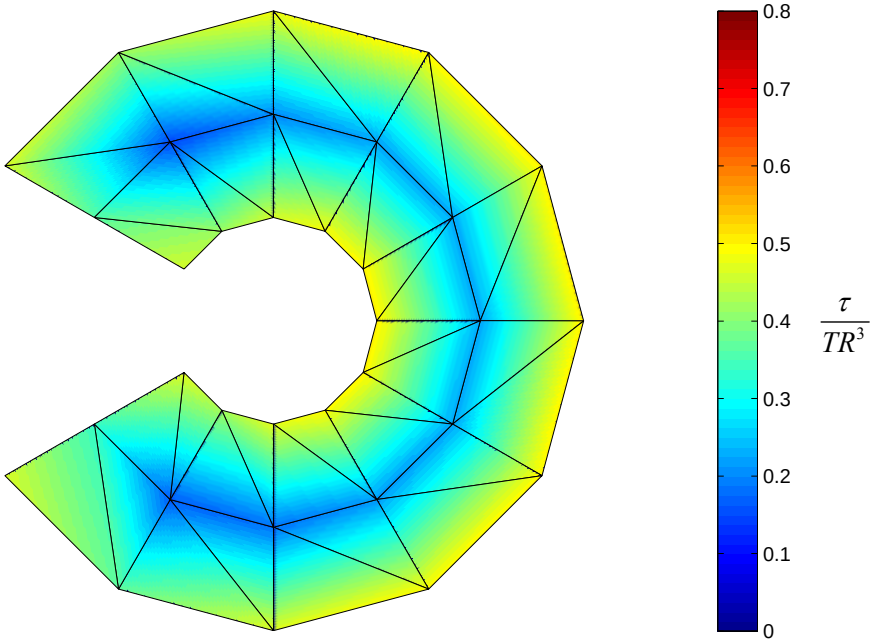

Figure 8. Distribution of the resultant shearing stress $\tau = \sqrt{\tau_{xy}^2 + \tau_{xz}^2}$, standard formulation.

Thin-walled open circular tube (Figure 9) was studied as a second example. Figures 10 and 11 demonstrate distribution of the resultant shearing stress τ obtained with the intrinsic and standard formulations, respectively. Table 3 shows comparison the maximum shearing stress $\tau_{\max}$ obtained using different mesh densities. Table 4 shows similar comparison of the torsional constant J. Practically exact results in Tables 3 and

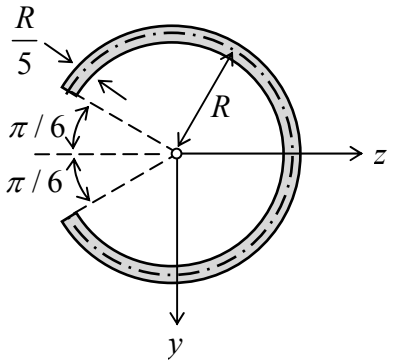

Figure 9. Thin-walled open circular tube.

Table 3. Comparison of the values of dimensionless maximum shearing stress $\tau_{\max} / TR^3$.

Element division	Present	Conventional
1×10	15,89	6,80
2×20	15,33	9,34
4×40	15,34	11,71
8×80	15,32	13,84
16×160	15,28	14,67
32×320	15,25	14,97
Practically exact result 15,21		
Thin walled theory approximation 14,32		

Table 4. Comparison of the values of dimensionless torsional constant J / R^4.

Element division	Present, equation(39)	Present, equation (53)	Conventional
1×10	0,0153	0,0140	0,0572
2×20	0,0143	0,0139	0,0259
4×40	0,0139	0,0138	0,0168
8×80	0,0137	0,0137	0,0144
16×160	0,0137	0,0136	0,0138
32×320	0,0136	0,0136	0,0137
Practically exact result 0,0136			
Thin walled theory approximation 0,0140			

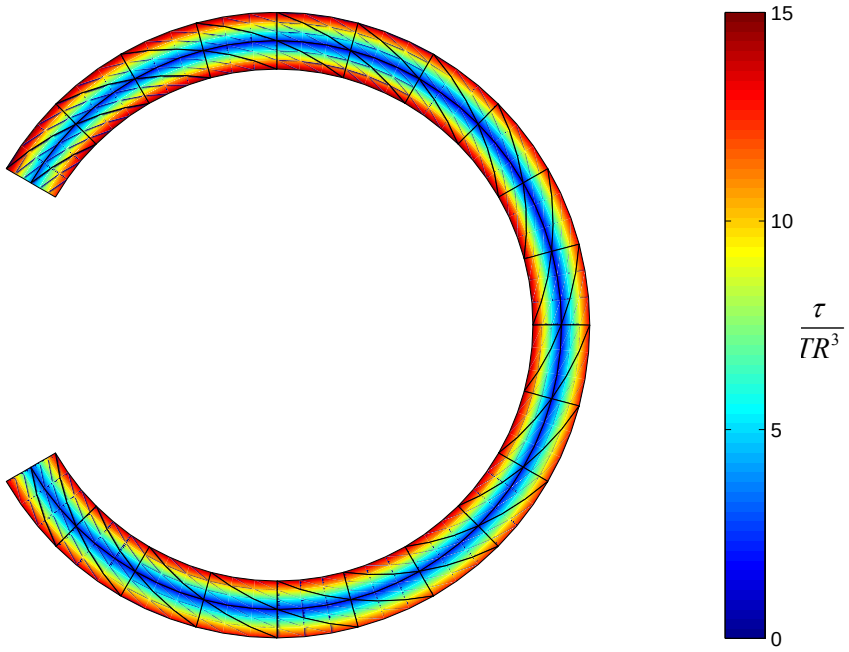

Figure 10. Distribution of the resultant shearing stress $\tau = \sqrt{\tau_{x\xi}^2 + \tau_{x\eta}^2}$, intrinsic formulation.

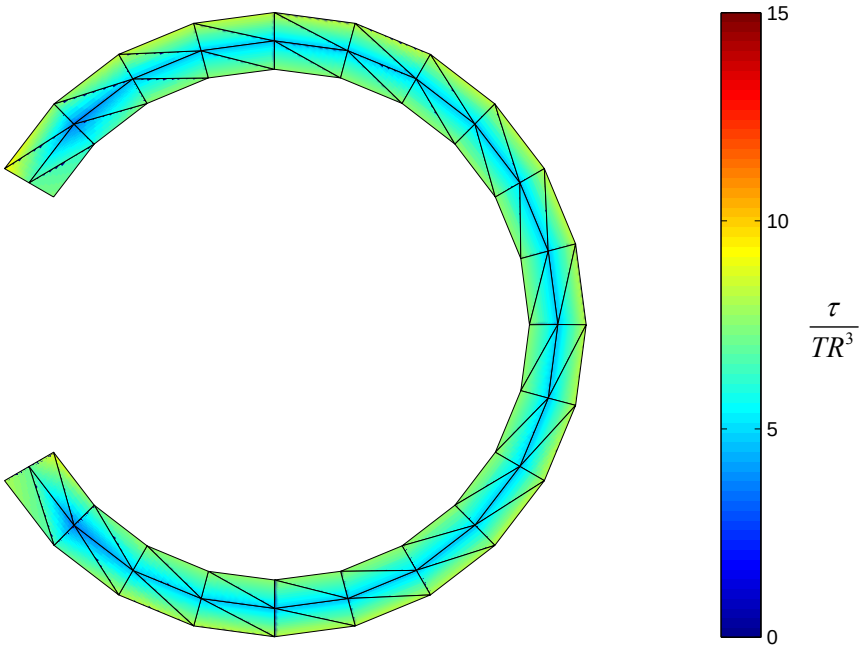

Figure 11. Distribution of the resultant shearing stress $\tau = \sqrt{\tau_{xy}^2 + \tau_{xz}^2}$, standard formulation.

4 were obtained using a very dense mesh (32×320) of biquadratic iso-parametric quadrilateral elements. Approximations based on thin walled theory are obtained using well known formulas

$$J=\frac{1}{3}lt^3=\frac{1}{3}\cdot\frac{5\pi}{3}R\cdot(\frac{R}{5})^3=\frac{\pi}{225}R^4=0,01396R^4,$$
$$\tau_{\max}=\frac{T}{J}t=T\cdot\frac{225}{\pi R^4}\cdot\frac{R}{5}=\frac{45}{\pi}\frac{T}{R^3}\approx14,32\frac{T}{R^3}. \qquad (59)$$

Here l is the length of the center line and t is the thickness of the layer.

L-shaped cross-section with rounded internal corner (Figure 12) was considered as a third example. In order to improve modeling of the stress concentration near the rounding, the elements forming a patch (intrinsic element patch) in the vicinity of the rounded corner were dealt with using intrinsic formulation and the other elements of the mesh using standard formulation. The spine of the corresponding intrinsic coordinates coincides with the circular rounding. Figure 13 demonstrates distribution of the shearing stress τ_{xy} obtained. For comparison the problem was also analyzed using a mesh of standard linear triangles. The corresponding stress distribution is shown in Figure 14. Table 5 shows comparison the maximum shearing stress $\tau_{\max}$ obtained using the two meshes and different densities. Table 6 shows similar comparison of the torsional constant J. Practically exact results in Tables 5 and 6 were obtained using a very dense mesh (32×192) of biquadratic iso-parametric quadrilateral elements.

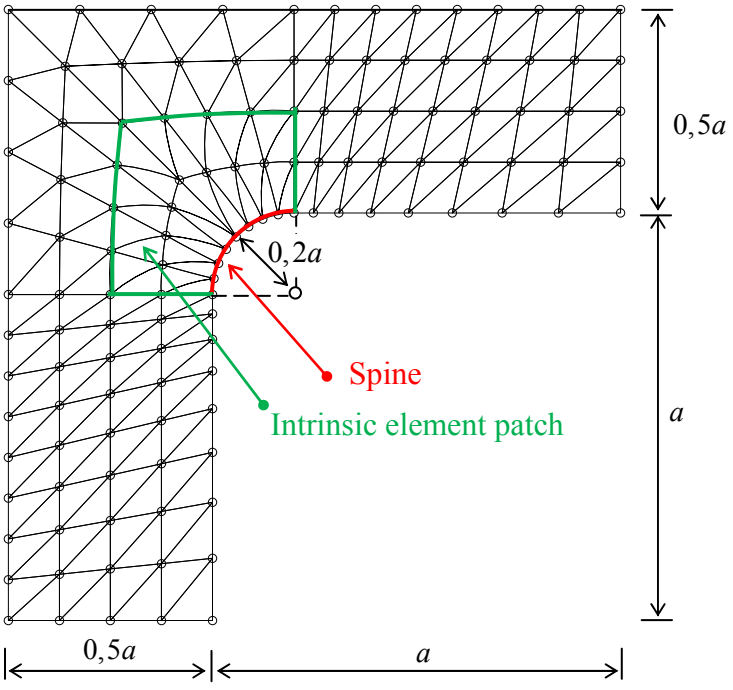

Figure 12. L-shaped cross-section with circular internal corner and a mesh of 192 elements.

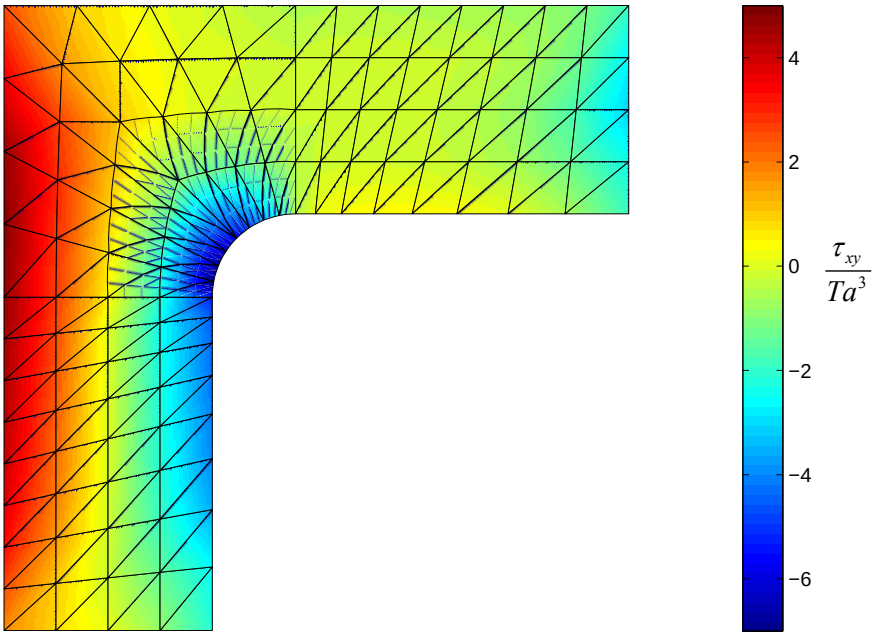

Figure 13. Dimensionless shearing stress $\tau_{xy}/(Ta^3)$ of the L-shaped cross-section, mesh with intrinsic element patch.

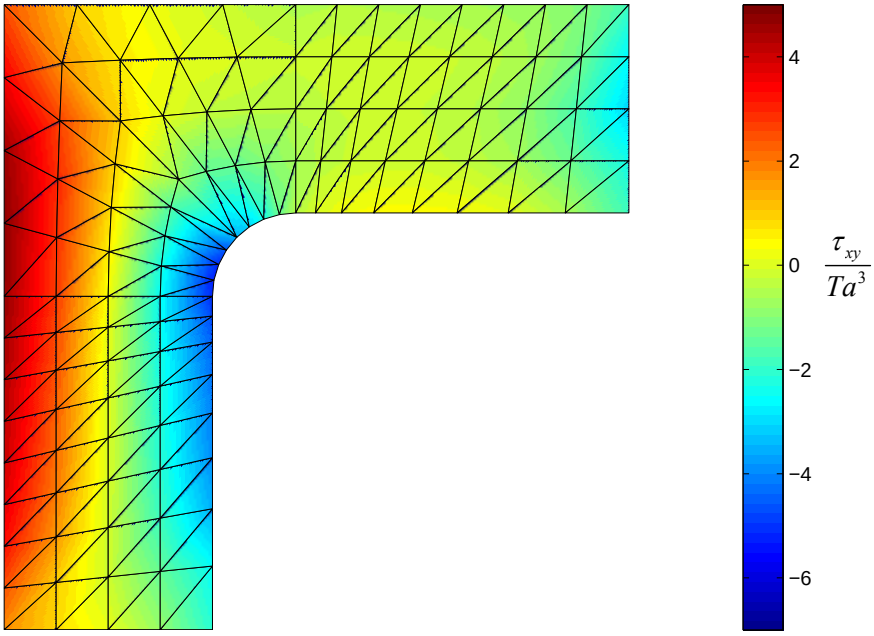

Figure 14. Dimensionless shearing stress $\tau_{xy}/(Ta^3)$ of the L-shaped cross-section, mesh of standard elements.

Table 5. Comparison of the values of dimensionless maximum shearing stress $\tau_{\max} / Ta^3$, L-shaped cross-section.

Element division	Mesh with intrinsic patch	Mesh with standard elements
2×12	7,43	4,32
4×24	7,70	5,65
8×48	7,73	6,52
16×96	7,71	7,02
32×192	7,69	7,32
Practically exact 7,69		

Table 6. Comparison of the values of dimensionless torsional constant J / a^4, L-shaped cross-section.

Element division	Mesh with intrinsic patch	Mesh with standard elements
2×12	0,1192	0,1257
4×24	0,1070	0,1087
8×48	0,1033	0,1037
16×96	0,1023	0,1024
32×192	0,1020	0,1021
Practically exact 0,1019		

Conclusions

Application of intrinsic coordinates in Saint Venant's torsion reveals some interesting analytical results for a rather general geometry. Further, use of the corresponding weak formulation with finite elements is found to increase the accuracy compared to the standard Cartesian coordinate approach.

Acknowledgement

We thank the reviewer of the article for comments which have led especially to a compact version of the differential equation for the warping function.

Appendix A

We will derive a useful auxiliary relationship to be applied in the article. Let us divide the rod cross-section A into two parts by a smooth curve c. A cylindrical surface having generators in the axial direction of the rod and going through c is further considered. The rod is now divided by the cylinder into two imaginary bodies. Let the shearing stress component on A at c perpendicular to c be denoted τ_{xn}. The force equilibrium in the axial direction for either of the two bodies is

$$L\int_c \tau_{xn}\,\mathrm{d}s = 0\,, \tag{A.1}$$

where L is the length of the cylinder. Dividing this by L gives

$$\int_c \tau_{xn}\,\mathrm{d}s = 0 \tag{A.2}$$

or in words: the line integral of the normal shearing stress over an arbitrary curve dividing the cross-section into two parts is zero.

References

[1] D.A. Anderson, J.C. Tannehill and R.H. Pletcher, *Computational Fluid Mechanics and Heat Transfer*, McGraw-Hill, New York, 1984.

[2] J. Paavola and E.-M. Salonen, 'Coping with curvilinear coordinates', *International Journal of Mechanical Engineering Education*, 26 (1998) 309-317.

[3] J. Paavola and E.-M. Salonen, 'Coping with curvilinear coordinates in solid mechanics', *International Journal of Mechanical Engineering Education*, 32 (2004) 1-10.

[4] J. Paavola and E.-M. Salonen, 'Coping with curvilinear coordinates in fluid mechanics', *International Journal of Mechanical Engineering Education*, 32 (2004) 11-17.

[5] S. Timoshenko and J.N. Goodier, Theory of Elasticity, second ed. Mc-Graw-Hill, New York, 1951.

Jukka Aalto, Juha Paavola, Eero-Matti Salonen
Aalto University, School of Engineering
Department of Civil and Structural Engineering
PO Box 12100, 00076 Aalto
jukka.aalto@aalto.fi, juha.paavola@aalto.fi, eero-matti.salonen@aalto.fi